# Local and Average Interphase Heat Transfer Coefficients in a Randomly Packed Bed of Spheres

BERNARD M. GILLESPIE, EDWARD D. CRANDALL, and JAMES J. CARBERRY

University of Notre Dame, Notre Dame, Indiana

Local and average heat transfer coefficients have been measured for a sphere in a randomly packed bed. A steady state technique was employed in which internally heated spheres were placed in a bed 35 in. deep and 12 in. sq. Air passed through the bed in downflow, the range of Reynolds numbers being from 120 to 1,700 based on the sphere diameter and the superficial velocity.

Average heat transfer coefficients have been measured at twenty-five positions permitting the assessment of the effect of position. An entrance region limited to the first two particle layers in the bed has been verified.

Distributions of the local heat transfer coefficient on the surface of a single sphere in the top layer and in the nineteenth layer of the bed have also been measured. These distributions indicate that a laminar boundary layer exists over portions of the sphere surface.

In the analysis and design of fixed bed reactors, adsorbers, etc., prudent account of interparticle and inter-intraphase transport events is desirable. This is particularly true in the case of the nonisothermal catalytic reactor wherein local surface reaction rates are governed by concentrations and a temperature dictated by transport of mass and heat between the bulk fluid phase and the sites of catalysis (*21, 27*).

Our concern in this instance is with interphase transfer of heat; that is, rates of heat transfer between a flowing fluid and the external surface of spheres comprising the fixed bed. As our ultimate interest resides in realizing greater understanding of the detailed structure of heat, mass, and momentum transfer in fixed beds, it follows that the initial inquiry must be focused upon local transfer rather than overall integral coefficients.

## BACKGROUND

Interphase transport in fixed beds may be expressed in the following terms:

### Type I.

Overall, integral coefficients determined by measuring net overall rates and inlet-outlet concentrations/temperatures. The results are commonly expressed as $j$ factors or Nusselt numbers correlated with Reynolds and fluid property groups. For mass transfer, a vast literature exists (*2, 5, 6, 7, 15, 20*). Overall interphase heat transfer coefficients have also been measured, duly correlated and discussed (*1, 10, 21, 25, 26*).

### Type II.

Average interphase coefficients have been determined for single particles immersed in a fixed bed of inert partner particles. This level of inquiry is free of gross end effects, radial velocity variations, etc., which plague interpretation of Type I data. Some Type II data results have been reported for mass transfer by Thatcher (*23*), Thoenes and Kramers (*24*), and recently by Rhodes and Peebles (*19*).

### Type III.

Local transfer coefficients for a single particle immersed in a bed of inert neighbors may be measured. Thus for a sphere, the variation of $k_g$ or $h$ might be measured as a function of angle from stagnation as has been commonly done in studies of transport to or from a sphere isolated in a free stream. This Type III level of inquiry provides in principle a much more detailed picture of the transport event. For local mass transport Rhodes and Peebles (*19*) provide data while Wadsworth (*25, 26*) reports local interphase heat transfer data for packed spheres at very high Reynolds numbers. An investigation complimenting ours has been in progress and the results for local mass transport between a flowing liquid and a sphere immersed in a fixed bed will shortly be made available (*13*). Not unrelated to this inquiry is the extensive work of Professor Pfeffer of City College of New York who is studying the influence of simple networks of noncontacting neighboring inert spheres upon local dissolution rates of a test sphere (*18*).

## SCOPE AND INTENT OF PRESENT INQUIRY

Our prime concern is the gas-solid fixed bed network. The average (Type II) and local (Type III) heat transport coefficients were measured for 1 in. diameter metal spheres immersed in a bed of 1 in. cork spheres. Air at room temperature flowed through the bed at Reynolds numbers between 120 to 1,700, based upon superficial velocity.

Calibration of the measuring techniques required additional measurements of average and local heat transfer coefficients for each test sphere situated in an unpacked wind tunnel (isolated sphere). These data are reported in the next section.

Several unresolved questions pertaining to fixed beds inspired the present study:

1. Since the early fixed bed velocity profile studies of Smith and his students (*22*) revealed unusual departures from plug flow, it could be anticipated that velocity dependent transport coefficients would display a radial dependency. Therefore, we sought to determine that de-

Bernard Gillespie is with Mobil Oil Corporation, Paulsboro, New Jersey.

pendency.

2. Entrance effects could also be anticipated. The question of precisely how many particle layers had to be passed before uniform behavior at a given radius is found had to be answered.

3. For a given sphere at a particular point in a fixed bed, how is the heat transfer coefficient distributed in its magnitude as a function of angle from stagnation?

4. What is the effect of repacking a bed in a random fashion upon average and local coefficients?

5. Finally, it was hoped that the detailed local coefficient data might clearly lend or deny support to a theoretically derived $j$ factor for fixed beds (*2, 17*). This model visualizes the successive development and destruction (through void cell mixing) of a laminar boundary layer at the fluid-solid interface. Diffusion within this series of boundary layers would thus account for interphase transport (*2*). While the simple model cited proved surprisingly faithful to experimental overall coefficient data, its very success prompts one to seek more precise and detailed confirmation.

## APPARATUS AND EXPERIMENTAL DETAILS

### Wind Tunnel

A vertical single pass wind tunnel was employed in these experiments. The upper section of the tunnel established a uniform velocity profile at the top of the working section and reduced the relative intensity of turbulence in the entering air. The working section which was 12 in. sq. and 35 in. long contained the packed bed during the measurements. Terminal boards and selector switches to accommodate the electrical circuits were mounted directly on the working section to facilitate its removal to repack the bed. The two sections below the working section reduce the area of flow to three inches in diameter to permit flow measurements to be made using a Pitot tube and micromanometer. The bottom section of the tunnel was connected to the suction side of a centrifugal blower. The air velocity was varied by changing the voltage applied to a ½ horsepower AC/DC motor thereby changing the motor speed. With the packing in the working section, a range of superficial velocities from 0.25 to 3.5 ft/sec. could be attained. This corresponds to a Reynolds number range of 120 to 1,700 when the Reynolds number is based on sphere diameter and superficial velocity.

### Sphere for Average Heat Transfer Coefficients

Figure 1 presents the details of construction of the spheres used to measure average heat transfer coefficients. Brass ball bearings of 1 in. were machined to hold a spherical heater and a surface thermocouple for this part of the work. The spherical heater consisted of approximately 5 ft. of 30 gauge copper magnet wire wrapped on the surface of a ⅜ in. aluminum ball. Details for the method used to fabricate these heaters are given elsewhere (*1*).

Two extra leads were soldered to the heater wire very close to the heater. This permitted the voltage drop across the heater to be measured directly in order to calculate the rate of heat generation. A copper-constantan thermocouple was soldered to the surface of the brass sphere and the leads from the thermocouple were passed along the shallow trough shown in the figure and then along the stainless steel support rod. The reference junction of this thermocouple was positioned in the flowing air stream.

### Sphere for Local Heat Transfer Coefficients

Figure 2 reveals details of the sphere employed to measure local heat transfer coefficients. The body of the sphere and the flux meter were both of bronze. The details of the flux meter are presented in the inset of the figure. The small air gap between the flux meter and the body of the sphere eliminated conduction of heat between the meter and the sphere body. Thus the temperature difference across the plug established the value of the heat flux. The thermocouple junctions, which were attached to the flux meter with epoxy glue, were 0.001 in. thick and the wires were 36 gauge.

### Other Equipment

Air velocity was measured using a Pitot tube and a model MM-3 micromanometer.

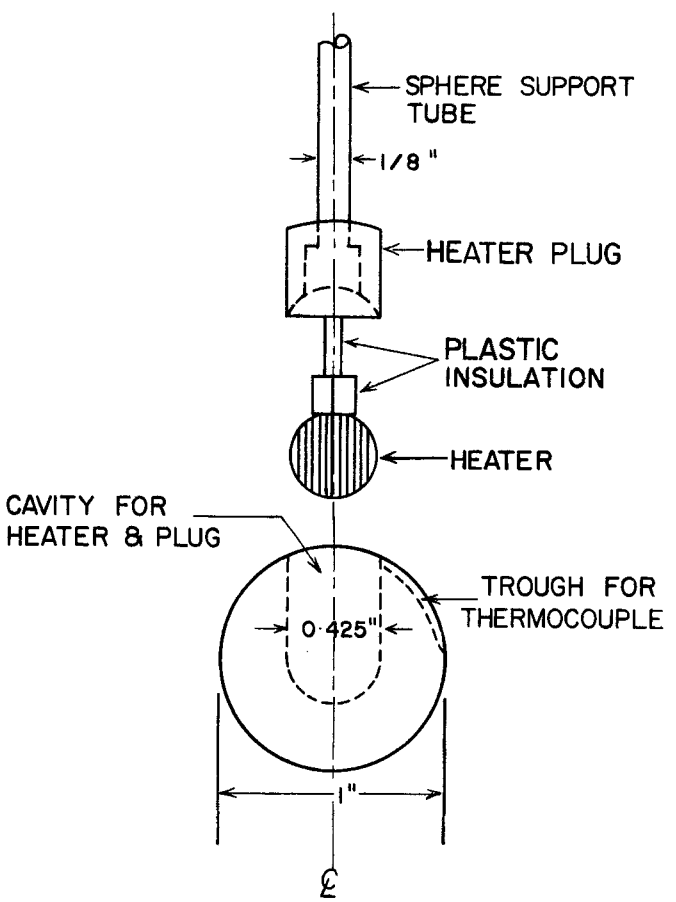


Fig. 1. Sphere construction for average heat transfer coefficients.

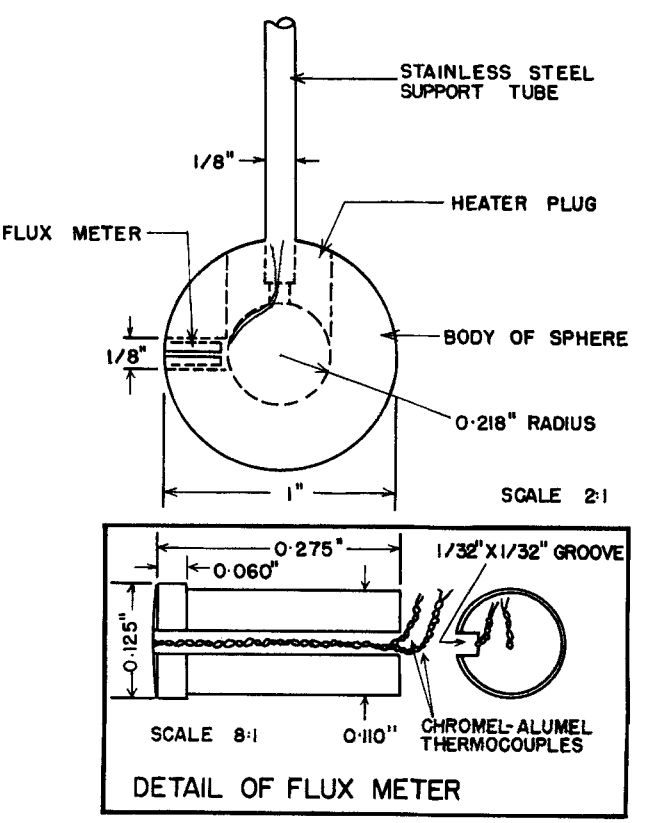


Fig. 2. Sphere construction for local heat transfer coefficients.

For the average heat transfer measurements the heater current was supplied by a 6v automotive battery connected in series with a rheostat, an ammeter and the sphere heaters. Heater current was read from the ammeter, a Weston Electric Model 44239. The voltage drop across each sphere heater was measured by one channel of a Honeywell Electronik 19 dual-channel recorder. The extra leads from the sphere heaters were connected through one of the selector switches to the recorder. The second channel of the recorder was used to measure the temperature difference between the sphere surface and the flowing air, once again through a selector switch. This channel also measured the air temperature by means of a thermocouple in the stream; the reference junction of this thermocouple was in an ice bath.

For the local heat transfer coefficients, the heater current circuit remained the same except that only one sphere heater was in the circuit. To calculate the local heat transfer coefficient, the heat flux and the temperature difference between the sphere surface and the air were required. A double pole–double throw switch, the center posts of which were connected to the surface thermocouple, enabled the differences in e.m.f. between the surface thermocouple and the interior couple and that between the surface thermocouple and the air thermocouple to be measured directly.

#### Preliminary Calibrations

The surface thermocouples of the five spheres used to measure average heat transfer coefficients were checked by placing each sphere in the vapor space of a boiling water bath, the reference junction being an ice water bath. The boiling point, corrected for barometric pressure (746 mm mercury after the brass scale correction had been applied), was 99.48°C., corresponding to a thermocouple output of 4.251 mv. based on a linear interpolation of the calibration given in Reference *12*. The five surface thermocouples tested read within .007 mv. of this value. The accuracy of the recorder used in the experimental runs was ± .01 mv. in this range.

The spheres for average heat transfer coefficients were further tested to determine whether they could satisfactorily reproduce the available data for average heat transfer coefficients for a single isolated sphere. Six runs were made with the spheres in the unpacked wind tunnel. The results are shown in Figure 3 and are compared with a recent correlation for single sphere heat transfer (*20*). Satisfactory agreement is evidently obtained between the present data and the correlation.

As discussed earlier the sphere used to measure local heat transfer coefficients contained a flux meter consisting of an insulated cylindrical rod with a thermocouple attached to each end. Calibration of the flux meter entailed the determination of the constant $K$ in the equation

$$q_r = K\Delta T \qquad (1)$$

Two independent methods were used: the first was based on integrating the local heat flux over the surface of the sphere and equating this to the average rate of heat loss per unit area of the sphere; the second was based on fitting the results of a series of measurements of the local heat transfer coefficient at the forward stagnation point to a correlation presented by Wadsworth (*25*). The details of the calibration procedures are presented in Reference 9. The value of the constant $K$ obtained from these methods was $1.17 \times 10^{-2}$ cal./sq.cm.-sec.°C. (the two methods differed by less than 2%).

The distribution of the local heat transfer coefficient for a single isolated sphere was measured at four flow rates. The results of these measurements are presented in Figure 4. The similarity of these distributions to those reported by Wadsworth (*25*) and by Carey (*3*) is worth noting.

## RESULTS FOR FIXED BED

As forced convection is implicitly assumed to be the only mode of heat transfer in this study, the total unimportance of a natural convection and radiation contribution must be demonstrated. Preliminary computations confirm the total absence of a radiation contribution while the Grashof numbers involved suggest a very negligible

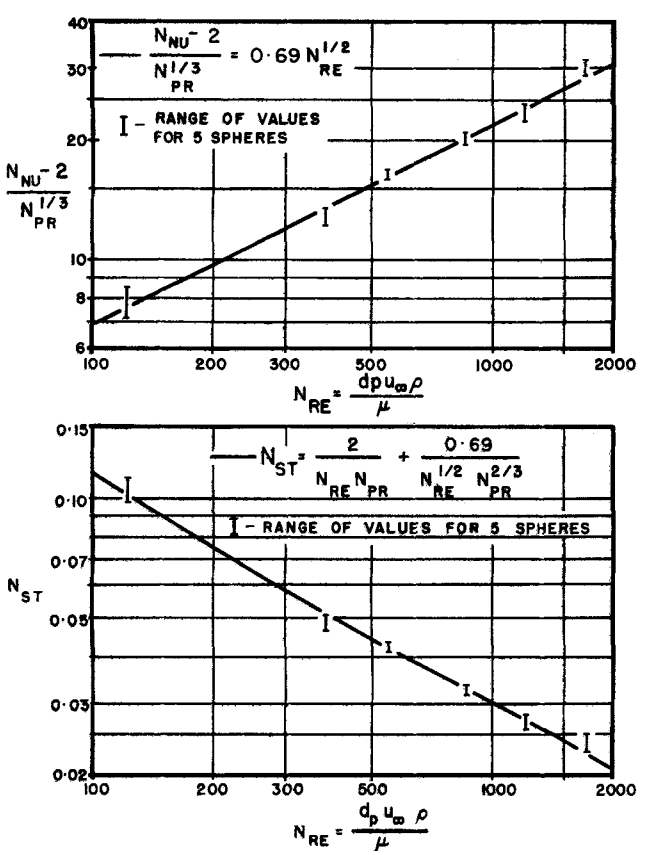


Fig. 3. Single sphere heat transfer coefficients (average values in unpacked conduits.)

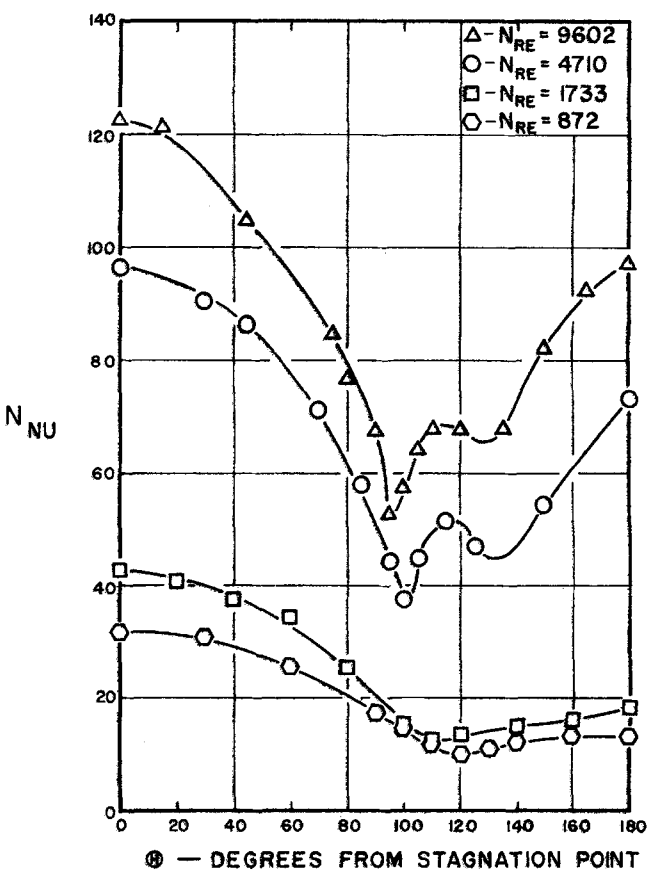


Fig. 4. Local Nusselt number distribution—single sphere in unpacked conduits.

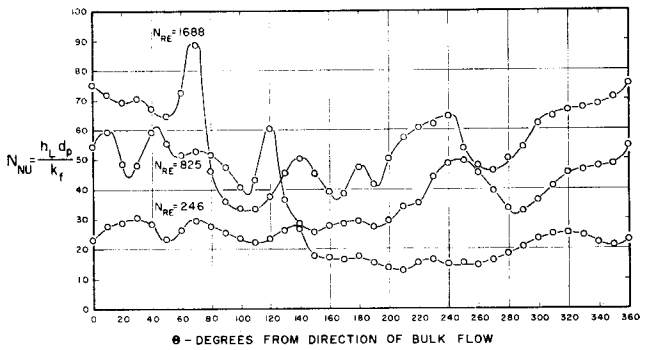


Fig. 5. Local Nusselt number—top layer, first packing.

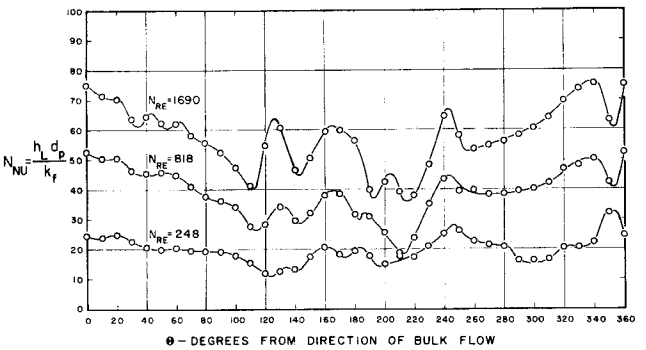


Fig. 6. Local Nusselt number—top layer, second packing.

contribution due to natural convection. Thus the measured coefficients may be considered forced convection heat transfer coefficients.

Detailed results of the average heat transfer coefficient study are presented elsewhere (9), while the resulting correlations are presented in the following section. The solid lines in Figure 11 represent the average coefficient correlation compared with averaged values of the local coefficient measurements.

Figures 5 through 10 present some of the local heat transfer coefficients measured in the packed bed. The measurements reported for the top layer were performed at a lateral position 2 in. from the wall. Three flow rates were examined at each position except one. Two packings of the bed were made at each position in order to assess the effect of repacking the bed.

Tabulated results are presented in Reference 9.

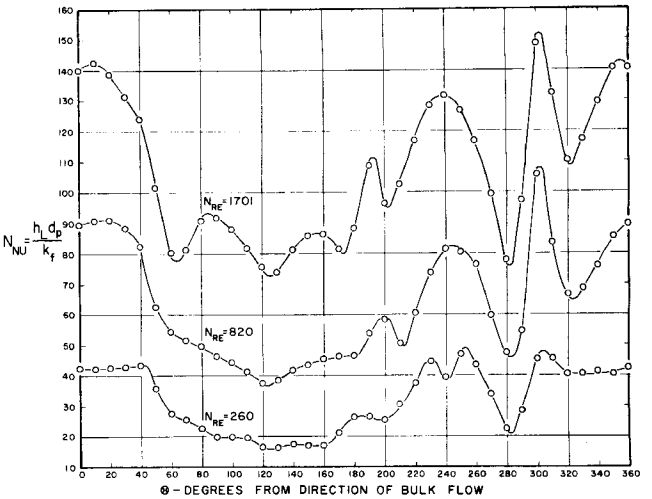


Fig. 8. Local Nusselt number—19th layer, at wall, second packing.

## DISCUSSION OF RESULTS

### Average Heat Transfer Coefficients; Single Sphere in Packed Bed

The data for each position in the bed were correlated by means of an equation of the form

$$N_{Nu} = A + a\ N_{Re}{}^{b} \qquad (2)$$

which correlates single sphere heat transfer data well. A linear least squares method was employed, in which integral values of $A$ from 0 to 10 were assumed and the best values of $a$ and $b$ were determined. The variance of the data was calculated for each value of $A$ and this variance was smallest for $A = 0$ indicating that, for these data, the best correlation was attained with an equation of the form

$$N_{Nu} = a\ N_{Re}{}^{b} \qquad (3)$$

The linear form of this equation was fitted to the data by the method of least squares.

### Effect of Depth

The most obvious feature of the measurements made at the different depths in the bed is the difference between the data for the top layer and that for the rest of the bed. The exponent on the Reynolds number, $b$ in Equation (3), is 0.48 for the top layer and between 0.63 and 0.69 for the layers beyond the second. The few measurements made in the second layer are intermediate. Additional evidence for the difference between the top layer and the

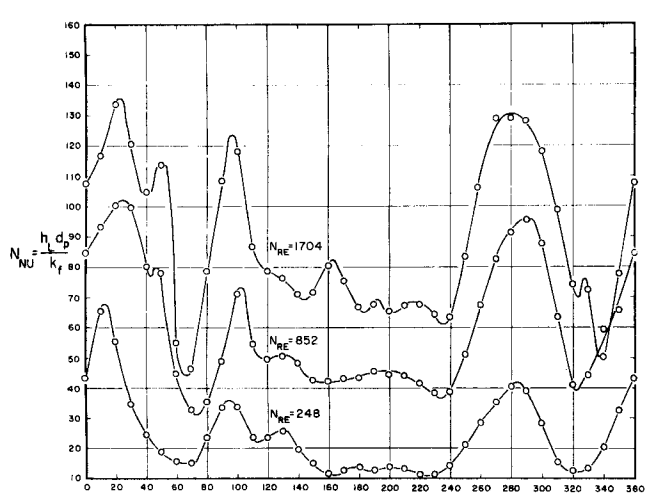


Fig. 7. Local Nusselt number—19th layer, at wall, first packing.

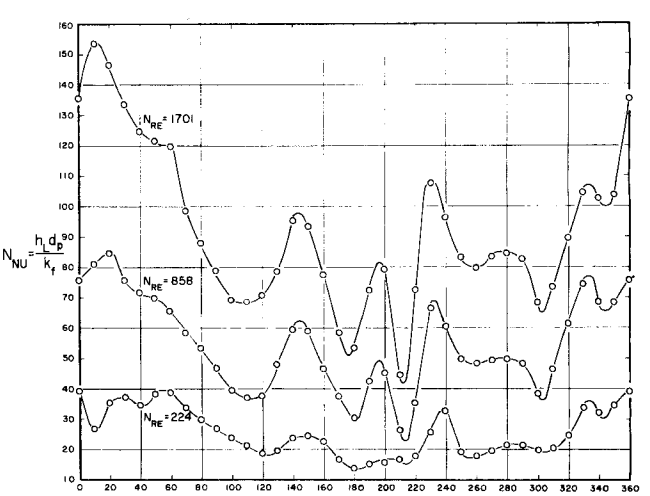


Fig. 9. Local Nusselt number—19th layer, centerline, first packing.

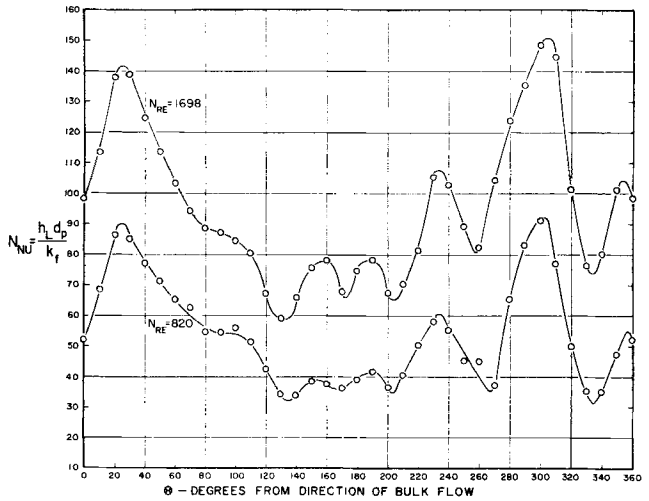


**Fig. 10. Local Nusselt number—19th layer, centerline, second packing.**

bulk of the bed will be discussed in connection with the local heat transfer measurements. Ignoring the top and the second layer measurements, the question can be examined, of whether the variations among the other correlations are statistically significant. To answer this question a procedure which is developed by Hald (*11*) was employed. The details of this analysis have been presented elsewhere (*9*) and will be omitted here. The conclusion reached is that for the third layer and beyond, the differences among the correlations are not significant. The effect of depth in the bed is restricted to an entrance region which is two particles deep. Beyond this depth the measurements do not depend on the depth.

#### Effect of Lateral Position

For each of the three regions in the bed (top layer, second layer, and bulk of the bed) the effect of lateral position was examined. This involves a comparison of the regression lines for these positions. A procedure for accomplishing this comparison has been developed in detail by Hald (*11*). Reference 9 presents the application of this analysis to these data. The conclusions for each of the lateral positions are that significant differences exist between the correlations. These differences are restricted to the intercepts of the regression lines, the slopes being indistinguishable. Table 1 presents the final correlations for the various positions in the bed. Standard deviations of the observed Nusselt numbers from the correlation at each position are also tabulated.

An interesting feature of Table 1 is that the value of $a$ increases as the wall is approached. This is probably caused by the increased flow rate and voidage near the wall as reported by Schwartz and Smith (*22*). An effort was made to relate the radial variation of $a$ with the velocity profiles measured by Schwartz and Smith (*22*). No success was realized in this attempt.

Table 1. Values of the Constant $a$ and Standard Deviations for the Correlation $N_{Nu} = a(N_{Re})^b$

| | Top layer $N_{Nu} = a(N_{Re})^{0.48}$ | | 2nd layer $N_{Nu} = a(N_{Re})^{0.58}$ | | Bulk of bed $N_{Nu} = a(N_{Re})^{0.65}$ | |
|---|---|---|---|---|---|---|
| | $a$ | $\sigma$ | $a$ | $\sigma$ | $a$ | $\sigma$ |
| Centerline | 1.37 | 8.7 | | | 0.63 | 9.8 |
| 2 in. from wall | 1.45 | 3.8 | | | 0.66 | 4.1 |
| 1 in. from wall | 1.44 | 3.1 | | | 0.67 | 5.3 |
| ¾ in. from wall | 1.55 | 6.0 | 1.11 | 4.6 | 0.73 | 3.8 |
| ½ in. from wall | 1.56 | 2.4 | 1.16 | 7.4 | 0.75 | 4.9 |

#### Local Heat Transfer Coefficients; Isolated Sphere

An examination of the local heat transfer results for single isolated spheres (Figure 4) will aid in the understanding of the packed bed results. For a single sphere the Nusselt number decreases from the forward stagnation point and reaches a minimum in the vicinity of 90°. This decrease is attributable to a laminar boundary layer increasing in thickness along this forward hemisphere. Beyond the 90° position the flow over the sphere surface experiences an adverse pressure gradient. This phenomenon is similar to the situation in a diverging cone where, if the angle is too large, separation may occur. For flow around a sphere separation occurs even at Reynolds numbers as low as twenty (*8*).

As the Reynolds number increases, the point of separation moves forward from the rear stagnation point and at Reynolds numbers greater than 450, the separation should occur at 104°. This separation angle is based on laminar boundary layer calculations, though there is considerable evidence that separation can occur forward of 104° and that the separation angle moves forward with increasing Reynolds numbers even beyond the 450 value quoted above (*14*).

From the forward stagnation point to the separation point the flow is described well by the boundary layer equations. Beyond this point though, external factors such as the method of support of the sphere, free stream turbulence, and the presence and form of container walls can affect the flow. In general, vortices are shed at a frequency which increases with Reynolds number, but at high Reynolds numbers it has been found that the flow may rejoin the sphere and begin to build up another boundary layer which subsequently separates (*26*). With this information about the flow pattern around a single isolated sphere, the variation of the local heat transfer coefficient around a single isolated sphere can be examined more closely. In Figure 4, for the lower Reynolds numbers, the heat transfer coefficient decreases on the forward hemisphere and, after separation, increases gradually again as the rear stagnation point is approached. For the runs at higher Reynolds numbers the decrease on the front half of the sphere is similar to the low flow rate measurements. However, after separation an increase in the heat transfer coefficient occurs. This is due to the wake flow recontacting the surface and, as can be seen, the flow rapidly separates again. After this separation the variation of the heat transfer coefficient follows the behavior for wake flow. This weak maximum in the heat transfer coefficient may result from the sphere support. The existence of such a maximum has also been reported by Wadsworth (*26*) at Reynolds numbers greater than 15,000, the lowest that he investigated. Two other aspects concerning the single sphere results are noteworthy. The position at which separation occurs, as denoted by the minimum in the heat transfer coefficient, moves forward on the sphere as the Reynolds number increases. Whether this is caused by the turbulence in the free stream or some other factor cannot be determined from the present results. The other aspect of the results which is not obvious from Figure 4 is that in the laminar boundary layer, the Nusselt number increases as the square root of the Reynolds number. While the isolated sphere measurements reported here are neither sufficient in number nor do they cover a wide enough range of Reynolds numbers to establish this relationship, the results of previous workers and the predictions of boundary layer theory must be considered as adequately establishing this relationship. This fact will be helpful in interpreting the packed bed results.

#### Local Heat Transfer Coefficients in Packed Bed

Before examining the results in any detail, an overall

comparison of the results in the top layer of the bed (Figures 5 and 6) with those in the 19th layer (Figures 7 to 10) suggests that for the top layer the local heat transfer coefficients are significantly lower than for the 19th layer, and the range of local Nusselt numbers (maximum value minus minimum value) in the top layer is much less than that in the 19th layer. That these two observations are related to the lower incident flow rate and the lower intensity of turbulence of the air entering the bed seems a logical speculation.

The effect of repacking the bed on the local heat transfer coefficient can be assessed from the figures. It is obvious that the distributions of the heat transfer coefficients for the two packings are not identical. Since the beds were randomly packed, this was expected. More striking, however, is the fact that the distributions for the two packings on the top layer of the bed are much more similar to each other than to any of the results in the 19th layer. One way of establishing the same conclusion is to examine the maximum and minimum values for the various distributions. For the first packing of the top layer, the local Nusselt numbers vary between 13 and 30 for the lowest flow rate, and between 33 and 89 for the highest. For the second packing the ranges are 12 to 32 and 35 to 86 These can be compared with the ranges for the 19th layer measurements at the wall of 11 to 68, 44 to 135 and 16 to 47, 74 to 148 for the low and high flow rates of the first and second packings. For the top layer the ranges change only slightly for the two packings whereas for the 19th layer more significant differences are seen for the two packings. Despite this the ranges are still more compatible between packings than between positions.

Some additional evidence of the effect of packing is available from the average values which were obtained by integrating the distribution of local coefficients over the surface of the sphere. Figure 11 shows the results of these integrations. The solid lines represent correlating

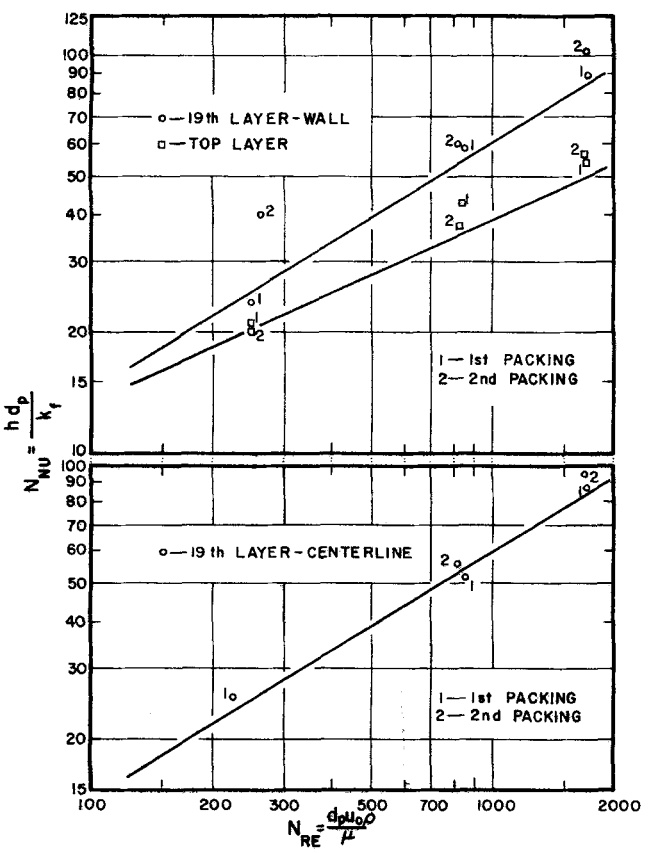


Fig. 11. Integrated average Nusselt number—lines represent correlation of measured average values.

relations found in the average coefficient study discussed earlier. It can be seen from this figure that the average coefficients secured by integration compare well for the two different packings. The worst deviation is for the measurements made at the wall in the 19th layer where the second packing shows a high trend. It must be realized that in the vicinity of the wall significant changes in the local packing arrangements are more likely than in the bulk of the bed. In addition, it should be noted that the integration of the local heat transfer coefficients in the bed was based on an assumption of symmetry which can only be justified in a probabilistic sense. Each of the measurements was assumed to be representative of a hemispherical shell in the direction normal to the bulk flow. The fact that the results agree so well with the correlations for the measured average coefficients (Figure 11) suggests that this assumption has some validity. The divergence of the integrated average values for the 19th layer wall measurements could in fact be caused not by any physical difference in packing but instead by expected asymmetry at the wall.

To summarize the effect of repacking the bed we can state that although the local heat transfer coefficient at a particular point on the sphere surface changes radically from packing to packing, the range of variation of the local heat transfer coefficient appears to be relatively insensitive to repacking.

The average heat transfer coefficients obtained by integrating the local values have been mentioned above in assessing the effect of repacking the bed. The results of these integrations are shown in Figure 11 compared with the correlation for the measured average values. The average Nusselt numbers were calculated from

$$\overline{N_{Nu}} = \frac{1}{4\pi R^2} \int N_{Nu}\, dA \qquad (4)$$

For a hemispherical shell

$$dA = \pi R \sin\theta\, (R d\theta) \qquad (5)$$

$$\overline{N_{Nu}} = \frac{1}{4} \int_0^{\pi} N_{Nu} \sin\theta\, d\theta \qquad (6)$$

The integral in Equation (6) was evaluated using Simpson's rule. That the results agree so well with the measured average values lends additional evidence to the validity of the packed bed measurements.

Examination of Figures 5 and 6 shows several interesting features. The regions from 290° to 360° in Figure 5, and 0° to 120° and 250° to 335° in Figure 6 possess the characteristics of laminar boundary layers. The decrease of the heat transfer coefficient in these regions is not so smooth as for the single sphere case, but this could be caused by secondary flows or could be the effect of the top packing support screen. Figure 6 in particular shows the forward movement of the separation point of the laminar boundary layer, from 120° at the lowest flow rate to 115° at the middle flow rate and to 112° for the highest.

Additional support for the existence of laminar boundary layer behavior in these regions can be realized by examining the dependence of the Nusselt number on the Reynolds number at a fixed angle. The Nusselt number–Reynolds number relationship in these regions is very close to the square root dependency which characterizes laminar boundary layers.

Outside the ranges of these laminar boundary layers, the variation of the heat transfer coefficient sheds little light on the flow pattern except to suggest its complexity. The maxima and minima are similar to those which occur in the wake of a sphere at higher Reynolds numbers but there is no obvious way to determine whether reattach-

ment of flow is occurring here. The region from 210° to 245° of Figure 6 would seem to indicate that the flow has reattached and is again building up a boundary layer on the surface. However this cannot be definitely established from the data.

The region from 80° to 130° in Figure 5 shows that the heat transfer is less for the highest flow rate than for the middle flow rate. A satisfactory explanation of this behavior has not been found. It is possible that this region represents a point of contact with another particle, but even then the result is unusual and especially for such a wide area of the surface. A plausible explanation is that the packing shifted in the vicinity of the measuring sphere between the time the measurements were made for the highest flow rate and the middle flow rate.

Figure 8 presents the results for the second packing at the wall in the 19th layer. A close examination of this figure is warranted if only because the average heat transfer coefficients calculated by integrating this distribution show the widest divergence from the measured average values. Examination of the region from 0° to 180° provides an excellent clue to the reason for this. Between 0° and 180° this distribution is quite similar to that of a single sphere. The boundary layer remains attached at the two lower flow rates until about 120°. Only at the higher flow rate does earlier separation occur. It is for the two lower flow rates that the average values differ considerably from the measured ones. Based on these two distributions, the reason for the differences may be an unusual packing arrangement in the bed which permits the laminar boundary layer to remain attached.

The local heat transfer coefficient measurements reported here can be compared with the mass transfer results of Rhodes and Peebles (*19*). Considering the widely different experimental techniques, the similarity of the distributions is satisfactory. One basic difference in the transport processes exists between these investigations: in this investigation, heat transfer could occur at the contact points between particles; whereas, for mass transfer the transport coefficient must be zero at a contact point. This could possibly be credited as an advantage to using the mass transfer technique.

The detailed examination of the distributions of the local heat transfer coefficient around a sphere in a randomly packed bed suggests the following:

1. The effect of repacking the bed is to change the distribution of the local heat transfer coefficient but repacking has little effect on the range of values (maximum-minimum) of the heat transfer coefficient for the sphere.
2. By examining the local heat transfer distribution, some information about the flow patterns around a sphere in a randomly packed bed can be inferred. In particular the existence of laminar boundary layer has been verified. Some expected similarities to the flow around a single sphere have been observed.
3. The entrance effect of the bed has been shown to result from two distinct differences between the local heat transfer coefficient on the top layer of the bed and in the bulk of the bed. The first of these, the lower absolute value of $h$ in the top layer, has been attributed to the lower incident flow rate. The second, the smaller range of variation of $h$ on a sphere in the top layer, has been attributed to the lower turbulence intensity in the entering air stream.

## CONCLUSIONS

1. The existence of an entrance region for the packed bed has been verified, and the effect of this region on the average heat transfer coefficient has been shown to be confined to the first two layers of particles in the bed.
2. An effect of lateral position on the average heat transfer coefficient in a packed bed has been observed. Higher heat transfer coefficients were found near the wall of the bed than in the center of the bed.
3. Local heat transfer coefficient measurements on the surface of a sphere in a packed bed have confirmed the effect of the entrance region and wall region. In addition, the local heat transfer coefficient distributions reveal that the lower flow rate and turbulence intensity of the entering air are probably both factors in the entrance effect.
4. Examination of the distribution of local heat transfer coefficients on the surface of a sphere in a randomly packed bed has yielded some insight into the boundary layer flows which exist in the bed. Laminar boundary layer behavior and the impingement of secondary flows may be deduced from the local heat transfer distribution.


## ACKNOWLEDGMENT

The authors express their gratitude to the National Science Foundation for a research grant to undertake this work. Bernard Gillespie gratefully acknowledges the financial assistance of a National Defense Education Act Fellowship.

The work reported is a part of the dissertation of Bernard Gillespie, submitted to the Graduate School, University of Notre Dame, in partial fulfillment of the requirements for the Ph.D.


## NOTATION

$A$ = constant in regression formulae, dimensionless
$A$ = surface area of sphere, sq.cm.
$a$ = constant in regression formulae, dimensionless
$b$ = constant in regression formulae, dimensionless
$d_p$ = particle diameter, cm.
$h$ = heat transfer coefficient, cal./sq.cm. sec. °C.
$h_i$ = local heat transfer coefficient, cal./sq.cm. sec. °C.
$K$ = proportionality constant defined by Equation (1), cal./sq.cm. sec. °C.
$k$ = thermal conductivity, cal./cm. sec. °C.
$k_f$ = thermal conductivity at film temperature, cal./cm. sec. °C.
$N_{Nu}$ = Nusselt number, dimensionless
$N_{Pr}$ = Prandtl number, dimensionless
$N_{Re}$ = Reynolds number, dimensionless
$N_{St}$ = Stanton number, dimensionless
$q_r$ = radial heat flux, cal./sq.cm. sec.
$R$ = sphere radius, cm.
$T$ = temperature, °C.
$u_o$ = superficial velocity, cm./sec.
$u_\infty$ = approach velocity, cm./sec.
$\Delta$ = difference, dimensionless
$\mu$ = viscosity, poises
$\rho$ = density, g./cc.
$\theta$ = angle from forward stagnation point, radians
$\sigma$ = standard deviation

## LITERATURE CITED


1. Baumeister, E. B., and C. O. Bennett, *AIChE J.*, **4**, 69 (1958).
2. Carberry, J. J., *AIChE J.*, **6**, 460 (1960).
3. Carey, J. R., *Trans. Am. Soc. Mech. Engrs.*, **75**, 483 (1953).
4. Denton, W. H., C. H. Robinson, and R. S. Tibbs, *Atomic Energy Research Establishment Rept. HPC-35*, Great Britain (1949).
5. Ergun, S. K., *Chem. Eng. Prog.*, **48**, 89 (1952).
6. Gaffney, B. J., and T. B. Drew, *Ind. Eng. Chem.*, **42**, 1120 (1950).
7. Gamson, M. B., G. Thodos, and O. A. Hougen, *AIChE J.*, **39**, 1 (1943).
8. Garner, F. H., V. G. Jensen, and R. B. Keey. Paper presented to Inst. Chem. Engrs., Birmingham, England (March, 1959).

9. Gillespie, B., Ph.D. dissertation, Univ. of Notre Dame, Indiana (1966).
10. Glaser, M. B., and G. Thodos, *AIChE J.*, 4, 63 (1958).
11. Hald, A., "Statistical Theory for Engineering Applications," pp. 579-584, John Wiley, New York (1953).
12. "Handbook of Chemistry & Physics," 35th Ed., p. 2369-2370, Chem. Rubber Publ. Co. (1953).
13. Jolls, K., and T. J. Hanratty, *Ind. Eng. Chem. Fundamentals*, to be published.
14. Linton, J., and K. L. Sutherland, *Chem. Eng. Sci.*, 12, 214 (1960).
15. McCune, L. K., and R. H. Wilhelm, *Ind. Chem. Eng.*, 41, 1124 (1949).
16. Meek, R. M. G., "Proceedings of the 1961-62 International Heat Transfer Conference," p. 769, A. Soc. Mech Engrs., New York (1963).
17 Mixon, F. O., and J. J. Carberry, *Chem. Eng. Sci.*, 13, 30 (1960).
18. Petzman, A., and R. Pfeffer, paper presented at AIChE Meeting, Detroit (1966).
19. Rhodes, J. M., and Q. N. Peebles, *AIChE J.*, 11, 481 (1965).
20. Rowe, P. N., K. T. Clayton and J. B. Lewis, *Trans. Inst. Chem. Engrs. (London)*, 43, T14 (1965).
21. Satterfield, C., N., and T. K. Sherwood, "Role of Diffusion in Catalysis," Addison Wesley, Reading, Pa. (1963).
22. Schwartz, C. E. and J. M. Smith, *Ind. Eng. Chem.*, 45, 1209 (1953).
23. Thatcher, Charles, Ph.D. thesis, Univ. Michigan, Ann Arbor, Mich.
24. Thoenes, D., and H. Kramers, *Chem. Eng. Sci.*, 8, 271 (1958).
25. Wadsworth, J., *Nat'l Res. Council of Canada Rept. No. MT-41* (1960).
26. ———, *Nat'l Res. Council of Canada Rept. No. MT-39* (1958).
27. Wilhelm, R. H., *Pure Appl. Chem.*, 5, 403 (1962).

*Manuscript received September 7, 1966; revision received July 31, 1967; paper accepted August 2, 1967.*

# Quasilinearization, Difference Approximation, and Nonlinear Boundary Value Problems

**E. STANLEY LEE**

**Kansas State University, Manhattan, Kansas**

**A finite difference method combined with the quasilinearization technique is used to solve the nonlinear two-point boundary value problems. This method does not have the stability problem connected with the marching integration techniques. A scheme which can be used to reduce the rapid access memory requirements of digital computers is also proposed. The steady state equations resulting from mass and energy balances in a tubular reactor with axial diffusion are solved by this method. With very poor initial approximations, only three to seven iterations are needed to obtain the correct answer.**

The two most frequently used methods for solving nonlinear two-point boundary value problems in ordinary differential equations are the trial and error method and the finite difference method. In the trial and error method, the values of the unknown initial conditions are assumed and are used with the given initial conditions so that the problem becomes an initial value problem. Thus, the generally used integration techniques, such as the Runge-Kutta method, can be used to obtain the solution. The final values that are obtained must agree with the given final conditions. Otherwise, some trial and error, or iterative procedure, must be devised to obtain better values for the assumed initial conditions. There are at least two difficulties associated with this procedure. The first one arises from the trial and error nature which is not suited for modern digital computers. Furthermore, actual experience has shown that the nonlinear boundary value problems encountered in engineering are frequently very sensitive to the errors of the unknown or assumed initial conditions. This difficulty becomes more severe if the problem to be solved has a large number of missing initial conditions.

The second difficulty arises from the stability problem associated with the generally used integration techniques such as the Runge-Kutta method, which is essentially a marching integration technique. To avoid this stability problem the finite difference method is used.

In the finite difference method, the original system of differential equations is approximated by a system of difference equations. There are several difficulties associated with this approach. The most important ones are the limited rapid access memory of current digital computers and the difficulty associated with the solution of a large system of nonlinear difference, or algebraic equations, that result from the original nonlinear differential equations.

In a recent paper [*1*], the quasilinearization technique was shown to be an effective tool to avoid the first difficulty associated with the trial and error procedure. This was accomplished by the combined use of linearization and the superposition principle. However, since the marching integration techniques were used in the above mentioned